

## Experimental and numerical analysis of elasto-plastic behaviour of notched specimen to tensile and compressive cyclic loading

Ganga Reddy C\* Dr. Shantharaja M\*\*

\*(Department of Mechanical Engineering, UVCE, Bangalore University, Bangalore-560001)

\*\* (Department of Mechanical Engineering, UVCE, Bangalore University, Bangalore-560001)

### ABSTRACT

The objective of the work was to estimate the elasto-plastic stress and strain behaviour at the root of the notch of an Al 6061 plate undergoing tensile and compressive cyclic loading by both experimental and numerical methods. This attempt to measured initial elasto-plastic stresses experimentally then verified by numerically. The various  $K_t$  values such as 2, 4 and 6 specimens were subjected to tensile test using a computerised universal testing machine. Numerical approach associated with body discretization and developed finite element model with sufficient degree of freedom to analyses elasto-plastic analysis of notched specimen. Experimental results show that analysis of three  $K_t$  notched specimens had similar behaviour of elasto-plastic behaviour but different magnitude. The experimental results compare well with the numerical results which are obtained during finite element analysis of notched specimens.

### I. Introduction

Recent years many researches [1] worked on interfacial crack and fracture of machine components. In other hand many engineering components contain geometrical discontinuous such as shoulders, keyways, oil holes and grooves, generally termed notches [2]. The notches are more prone to local stress and strain concentration when they are loaded condition. The stresses around notches are exceeding their yield limit even for nominal elastic stress [3]. The higher stress and strain concentration at notch does not impair the strength of the machine part, which made of a ductile material but the plastic deformation occur at the notch root. Further the notched machine part is subjected to cyclic loading the severity of plastic deformation more effective and it reduces the life of the components.

The linear rule is based on the assumption that the strain concentration factor is the same as the elastic stress concentration factor,  $K_t$ . The strain at notch root is expressed as  $\epsilon = K_t e$ , where  $\epsilon$  is plastic strain,  $K_t$  is stress concentration and  $e$  is elastic strain. Stephens et al. [4] suggest that this rule agrees well with measurements in plane strain situations, such as for circumferential grooves in shafts in tension or bending. Gowhari-Anaraki and Hardy [3] compared the calculated strains in hollow tubes subjected to monotonic and cyclic axial loading from the linear rule with predictions from finite element analyses. They predicated elasto-plastic deformation which was less than 50 % of experimental values [5].

Stowell [6] and Hardrath et al.[7] developed two equations to predict the elasto-plastic stress and strain behaviour at the peak stress of the specimens. The first of these was developed by Stowell [8] and modified by Hardrath and Ohman [9-10]. Two equations are used for predicting stress and strain at the notch root, elastic stress, stress concentration and nominal stress. These equations have been altered slightly for fatigue applications and used to estimate stress and strain histories at notch roots for cyclic loading. Although they developed equations successfully describing cyclic condition at the root of the notch but as per author knowledge which is not extended to experimental work. The objective of the work was to investigate effect of stress concentration factor on elasto-plastic behaviour of Al6061 ally by experimental and finite element technique.

### II. Experimental study

The experimental work was carried out for different stress concentration factors such as 1.75, 2.00, 2.25 and 2.50 to study the elasto-plastic behaviour. The material used was A-6061 aluminium alloy and the chemical composition is given Table 1.

Mg.	Si	Fe	Cu	Al
0.92	0.76	0.28	0.22	Bal.

The specimen dimensions were adopted as per the standards adopted by Zeng et.al.,[1], for their

work on elasto-plastic stress-strain behavior as shown in Fig. 1 and dimensions are given Table 2.

Table 2 Specimen Dimensions use in experiment				
Parameter	Dimension (in mm)			
	K <sub>t</sub>			
	1.75	2.00	2.25	2.50
<b>d</b>	9.23	7.10	5.25	3.50
<b>h</b>	4.00	4.00	4.00	4.00
<b>L</b>	60.32	60.32	60.32	60.32
<b>H</b>	41.28	41.28	41.28	41.28
<b>r</b>	11.11	11.11	11.11	11.11

The specimens with different notch radii were then fabricated from a larger sheet of Al 6061 by wire cutting method. The wire cut method was used as it gave a very accurate dimensional tolerance. A Universal Testing Machine (UTM) was used to perform tensile testing of the fabricated specimens. The specimens with different stress concentration factors were subjected to tensile load till fracture. The resultant broken specimens was subjected to fracture analysis using Scanning Electron Microscope (SEM) analysis.

As the specimen had a smooth surface, it had to be roughened at the ends, so that it could be held in the grippers effectively without slipping. A strain gauge was mounted on the specimen at the vicinity of the notch root, as the mounting of the strain gauge exactly at the notch root was difficult, owing to very small width of the plate and curvature of the notch. The strain gauge was mounted on the specimen at the point shown in the Fig. 1.

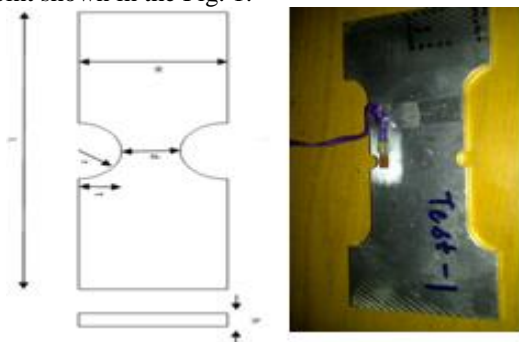


Fig. 1 Test specimen for elasto-plastic studies

### III. Numerical Analysis

For this research work geometrical models of different stress concentration factors were created using ANSYS as a platform. The models have varying notch radius (r), such that K<sub>t</sub> values obtained were 1.75, 2, 2.25 and 2.50. The thickness of the specimen was fixed at 4mm so as to prevent buckling of the specimen under tensile and compressive loading. SOLID186 element was selected for analysis of notch root, which exhibits quadratic displacement behaviour as shown in Fig. 2. The element is defined by 20 nodes having three degrees of freedom per node: translations in the nodal x, y,

and z directions. The element supports plasticity, hyper-elasticity, creep, stress stiffening, large deflection, and large strain capabilities. The meshing and constraints of tensile specimen is shown in Fig. 2

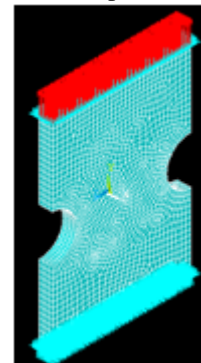


Fig. 2 FE Model for elasto-plastic studies

## IV. Results and Discussion

### 4.1 Numerical results

The stress and strain values obtained at the notch root by numerical analysis, is plotted for all the four K<sub>t</sub> values as shown in Fig. 3 (a-d). The stress strain variations obtained for the specimens conform to the standard stress strain variation of the Al6061 alloy material. As discussed in the previous chapter, the complete cycle was divided into 40 load steps. The corresponding stress and strain values are tabulated for each specimen.

The stress – strain values obtained from non - linear Finite Element Analysis (FEA) are plotted for each of the specimen bearing different K<sub>t</sub> values as shown in Fig. 3(a).

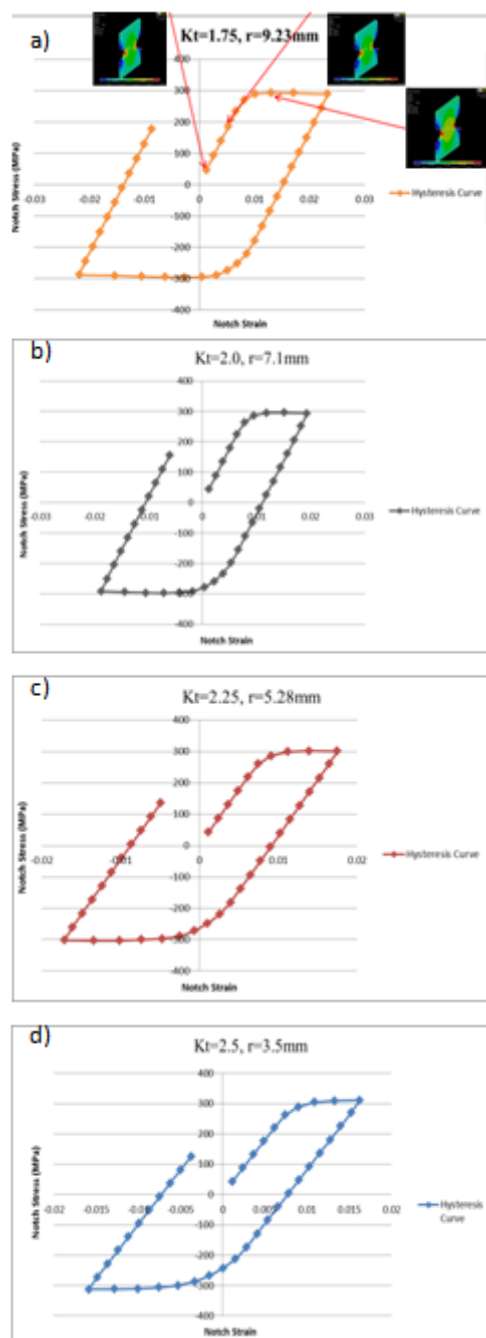


**Fig. 3 Hysteresis plot for different Kt a) 1.75, b)2.00, c)2.25 and 2.5**

For  $K_t = 1.75$ , it can be inferred from the Fig 3(a) that for the maximum tensile loading of 26.5kN , the corresponding maximum stress and maximum strain values are 289.12 MPa and 0.023256 respectively. For the maximum compressive loading of 26.5kN, the corresponding maximum stress and maximum strain values are 287.60 MPa and 0.02182 respectively.

For  $K_t = 2.00$ , it can be inferred from the Fig 3(b) that for the maximum tensile loading of 26.5kN, the corresponding maximum stress and maximum strain values are 293.47 MPa and 0.019289

respectively. For the maximum compressive loading of 26.5kN, the corresponding maximum stress and maximum strain values are 292.50 MPa and 0.018704 respectively.

For  $K_t = 2.25$ , it can be inferred from the Fig 3(c) that for the maximum tensile loading of 26.5kN , the corresponding maximum stress and maximum strain values are 300.86 MPa and 0.017479 respectively. For the maximum compressive loading of 26.5kN, the corresponding maximum stress and maximum strain values are 301.04 MPa and 0.017131 respectively.

For  $K_t = 2.5$ , it can be inferred from the Fig. 3(d) that for the maximum tensile loading of 26.5kN , the corresponding maximum stress and maximum strain values are 310.85 MPa and 0.016219 respectively. For the maximum compressive loading of 26.5 kN, the corresponding maximum stress and maximum strain values were 312.86 MPa and 0.015866 respectively.

From the plots obtained from the numerical analysis, it can be inferred that the stress at a given load point increases with increase in stress concentration factor. This is illustrated by the variation of maximum notch stress corresponding to load of 26.4kN with  $K_t$  as shown in the Fig.4.

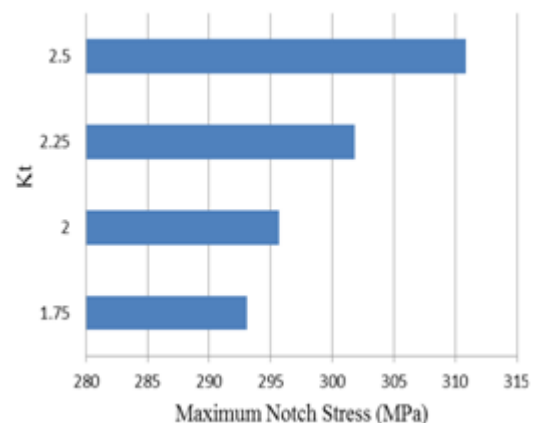


**Fig. 4 Variation of maximum notch stress with  $K_t$**

The maximum notch stress for specimens with  $K_t$  1.75, 2.00, 2.25 and 2.50 were found to be 293 MPa, 296 MPa, 302 MPa and 312 MPa respectively.

#### 4.2 Correlation of Numerical analysis and Experimental testing for tensile loading

The difference between mean of ANSYS and experimental values is - 0.000751 and the percentage error is - 8.07%. The difference between the median of ANSYS and experimental values is - 0.001281 and the percentage error is -17.164%. The percentage error in standard deviation is -3.037%.

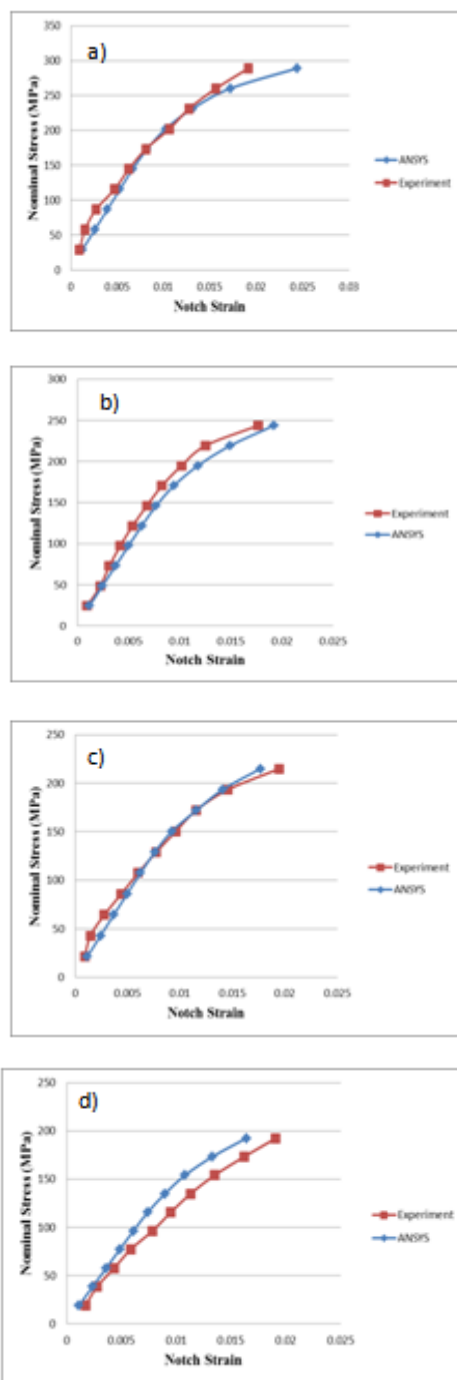


**Fig 5 : Experiment and numerical tensile results**  
 a)  $K_t = 1.75$ , b)  $K_t = 2.00$ , c)  $K_t = 2.25$  and d)  $K_t = 2.5$  respectively

Fig. 5 (a) shows the difference between mean of ANSYS and experimental values is -0.000292 and the percentage error is -3.57%. The difference between the median of ANSYS and experimental values is -0.00129 and the percentage error is -18.41%.

Fig. 5 (b) shows the difference between mean of ANSYS and experimental values is -0.000292 and the percentage error is -3.57%. The difference

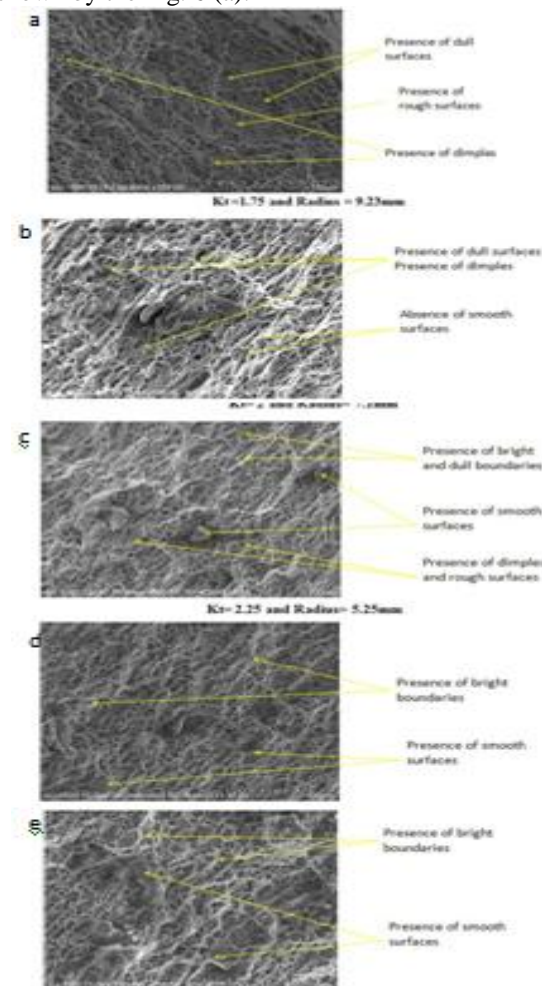
between the median of ANSYS and experimental values is -0.00129 and the percentage error is -18.41%.

Fig. 5 (c) shows the difference between mean of ANSYS and experimental values is 0.000087 and the percentage error is 1.108%. The difference between the median of ANSYS and experimental values is -0.000151 and the percentage error is -2.185%.

Fig. 5 (d) shows the difference between mean of ANSYS and experimental values is 0.00135 and the percentage error is 18.02%. The difference between the median of ANSYS and experimental values is 0.00192 and the percentage error is 28.486%.

### 4.3 Fracture surface studies

The SEM analysis done on the specimen with  $K_t = 0$  and notch radius 0 mm reveals the fracture type. The fracture occurs in a more ductile compared to other specimens with  $K_t$  values 2.50, 2.25, 2 and 1.75. This is shown by the absence of smooth surfaces and presence of dull intergranular surface and boundaries. The presence of more prominent dimples and rough surface reveals ductile nature of the fracture. The figure obtained from SEM at magnification 550X is shown by the Fig. 6 (a).



**Fig 6 : Fracture surface of a)  $K_t = 0$ , b)  $K_t = 1.75$ , c)  $K_t = 2.00$ , d)  $K_t = 2.25$  and e)  $K_t = 2.5$  respectively**

The SEM analysis done on the specimen with  $K_t = 1.75$  and notch radius 9.23mm reveals the fracture type. The fracture occurs in a relatively more ductile way than the specimens with  $K_t$  values 2.50, 2 and 1.75. This is shown by the absence of smooth surfaces and presence of dull intergranular surface and boundaries. The presence of more prominent dimples and rough surface reveals ductile nature of the fracture. The figure obtained from SEM at magnification 550X is shown by the Fig. 6(b).

The SEM analysis done on the specimen with  $K_t = 2$  and notch radius 7.1mm reveals the fracture type. The fracture occurs in a ductile way than the specimens with different  $K_t$  values 2.25 and 2.50. This is shown by the presence of smooth surfaces and presence of bright and dull inter-granular boundaries. The presence of dimples, rough surfaces show that it's a characteristic feature of ductile fracture relative to the specimens with  $K_t$  values 2.50 and 2.25. The figure obtained from SEM at magnification 550X is shown by the Fig. 6(c)

The SEM analysis done on the specimen with  $K_t = 2.25$  and notch radius 5.25mm reveals the fracture type. The fracture occurs in a relatively less brittle way than the specimens with different  $K_t$  values 2 and 1.75. This is shown by the presence of smooth surfaces and presence of bright intergranular boundaries. The figure obtained from SEM at magnification 550X is shown by the Fig. 6(d)

The SEM analysis done on the specimen with  $K_t=2.5$  and notch radius 3.5mm reveals the fracture type. The fracture occurs in a relatively more brittle way than other specimens with different  $K_t$  values and notch radius. This is shown by the presence of smooth surfaces and presence of bright intergranular boundaries. The figure obtained from SEM at magnification 550X is shown by the Fig. 6(e)

## V. Conclusion

The notch stresses, on application of maximum load, computed for  $K_t$  1.75, 2, 2.25, 2.5 are 289 MPa, 294 MPa, 301 MPa, 311 MPa respectively, which shows that as  $K_t$  increases from 1.75 to 2.5 in steps of 0.25, the notch root stress for the same load increases by approximately 2%. Also the notch strain obtained at maximum load decreases by 15% with the increase in  $K_t$ .

The standard deviation between the experimental testing and numerical analysis for the  $K_t$  values 1.75, 2, 2.25 and 2.5 obtained are 0.0071, 0.00597, 0.00575 and 0.00542 respectively. From these values it is evident that the deviation between the experimental results and numerical results is consistent. The t-scores obtained for  $K_t$  1.75, 2, 2.25 and 2.5 are 0.236, 0.109, - 0.034 and -0.557 respectively. The t-probability values obtained from the t-scores and the degrees of freedom are 0.8158, 0.9140, 0.9734 and 0.5842 for  $K_t$  1.75, 2, 2.25 and

2.5 respectively. This is shown from the fractography analysis of the SEM images of the fractured surface at the notch root. From the images it is evident that the nature of fracture is more brittle as  $K_t$  increases.

## References

- [1] Glinka G., "Energy density approach to calculation of inelastic strain-stress near notches and cracks", Engineering Fracture Mechanics, 1985, pp. 485-508.
- [2] Z Zeng "Elasto-plastic stress and strain behaviour at notch roots under monotonic and cyclic loadings", 10 January 2001, pp. 287-300.
- [3] Gowhari-Anaraki, A. R. and Hardy, S. J. "Low cycle fatigue life predictions for hollow tubes with axially loaded axisymmetric internal projections", 1991, pp.133-146.
- [4] Stephens, R. I. Fatemi, A. Stephens, R. R. and Fuchs, H. O., "Metal Fatigue in Engineering", 2nd edition, (John Wiley, New York) 2000, pp. 2-20.
- [5] John H. Crews, Jr "Elastoplastic stress-strain behaviour at notch roots in sheet specimens under constant-amplitude loading", NASA TECHNICAL NOTE, NASA TN D-5253, June 1969, pp. 4-32
- [6] Stowell, Elbridge Z., "Stress and Strain Concentration at a Circular Hole in an Infinite Plate", NACA TN 2073, 1950, pp. 18-51
- [7] Hardrath, Herbert F. and Ohman Lachlan, "A Study of Elastic and Plastic Stress Concentration Factors Due to Notches and Fillets in Flat Plates", NACA Rep. 1117, 1953. (Supersedes NACA TN 2566), pp. 5-16.
- [8] Stowell, Elbridge Z., "Stress and Strain Concentration at a Circular Hole in an Infinite Plate", NACA TN 2073, 1950, pp. 18-51.
- [9] Sharpe Jr, W. N. ASME 1993 "Nadai lecture—elastic plastic stress and strain concentrations", Trans. ASME, J. Engng Mater. Technol., 1995, pp. 1-7.
- [10] John H. Crews, Jr "Elasto-plastic stress-strain behaviour at notch roots in sheet specimens under constant-amplitude loading", NASA TECHNICAL NOTE, NASA TN D-5253, June 1969, pp. 4-32